Supporting Information: Competitive Adsorption of Xylenes at Chemical Equilibrium in Zeolites

Sebastián Caro-Ortiz,[†] Erik Zuidema,[‡] Marcello Rigutto,[‡] David Dubbeldam,[¶] and Thijs J. H. Vlugt[*,†]

[†]*Engineering Thermodynamics, Process & Energy Department, Faculty of Mechanical, Maritime and Materials Engineering, Delft University of Technology, Leeghwaterstraat 39, 2628 CB Delft, The Netherlands*

[‡]*Shell Global Solutions International B.V., PO Box 38000, 1030 BN, Amsterdam, The Netherlands*

[¶]*Van 't Hoff Institute of Molecular Sciences, University of Amsterdam, Science Park 904, 1098 XH Amsterdam, The Netherlands*

E-mail: t.j.h.vlugt@tudelft.nl

This Supporting Information contains: All force field parameters used in this work; the change of ideal gas free energy $\Delta G^{\text{ideal}}_{A \leftrightarrow B}$ of the reactions $A \leftrightarrow B$ computed using tabulated data for the reactions considered in this work; details regarding the calculations of entropy and enthalpy changes due to adsorption using multiple linear regression; the computed composition of the mixture of xylene isomers at chemical equilibrium as a function of pressure at 523 K; the computed fugacity coefficients of xylene isomers as a function of pressure at 532 K; the computed heats of adsorption of xylene isomers at infinite dilution in the zeolite types considered in this work; the computed changes of free energy, enthalpy, and entropy due to the transfer of a xylene molecule between the bulk phase at chemical equilibrium and the zeolite types considered in this work; the computed densities of the mixtures of xylene isomers as a function of pressure at 523 K.

Table S1: Force field parameters of the guest-guest interactions. Lennard-Jones parameters are listed. The reader is referred to the original publication of the force field for details.[S1]

Molecule	Pseudo-atom	ϵ/k_B / [K]	σ / [Å]	q / [e]
Xylenes	C	21.0	3.880	0
	CH	50.5	3.695	0
	CH_3	98.0	3.750	0

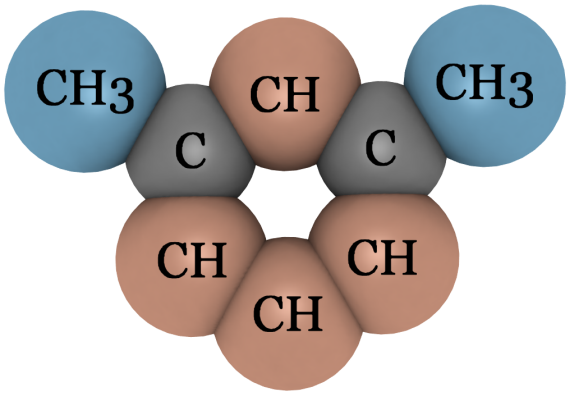

Figure S1: Schematic representation of *m*-xylene for the TraPPE-UA[S1] force field. Pseudo-atom labels use the notation of Table S1.

Table S2: Force field parameters of the host-guest interactions. Lennard-Jones parameters are listed. Partial charges for Si and O atoms are included in the original force field. Electrostatic interactions are not considered in this work. The interactions between different host-guest atom types are obtained using Lorentz-Berthelot mixing rules.[S2] The reader is referred to the original publication of the force field for details.[S3]

Pseudo-atom	ϵ/k_B / [K]	σ / [Å]	q / [e]
Si	22.0	2.3	+1.50
O	53.0	3.3	-0.75

Table S3: Helium void fraction and gravimetric surface area computed using iRASPA,[S4] unit cell parameters, and amount of unit cells considered for the simulations of each zeolite framework used in this work. *Maximum diameter of a sphere that can be included in the zeolite framework.[S5]

Zeolite type	Helium void faction / [-]	Surface area / [m^2/g]	Unit cells	Unit cell dimensions / [Å]			Unit cell angles / [°]			Max. diam. sphere* / [Å]
				a	b	c	α	β	γ	
FAU	0.494	1212.8	2 x 2 x 2	24.345	24.345	24.345	90	90	90	11.24
MWW	0.395	965.1	3 x 3 x 2	14.390	14.390	25.198	90	90	120	9.69
AFI	0.291	602.4	3 x 3 x 4	13.8271	13.8271	8.58035	90	90	120	8.3
MEL	0.309	736.1	2 x 2 x 3	20.270	20.270	13.459	90	90	90	7.72
MOR	0.309	1002.9	2 x 2 x 4	18.256	20.534	7.542	90	90	90	6.7
BEA	0.415	1063.5	3 x 3 x 2	12.632	12.632	26.186	90	90	90	6.68
MRE	0.172	354.2	4 x 2 x 2	8.257	14.562	20.314	90	90	90	6.36
MFI	0.265	657.5	2 x 2 x 3	20.090	19.738	13.142	90	90	90	6.36
MTW	0.238	537.4	2 x 6 x 3	25.552	5.256	12.117	90	109.312	90	6.08

The change of ideal gas free energy $\Delta G^{\text{ideal}}_{A\leftrightarrow B}$ of a reaction $A \leftrightarrow B$ is computed with tabulated enthalpies and entropies of formation using:[S6]

$$\begin{aligned}\Delta G^{\text{ideal}}_{A\leftrightarrow B} = \Delta H^{o}_{f,B} - \Delta H^{o}_{f,A} + \int_{298K}^{T} \Delta C_{p,A\leftrightarrow B} dT \\ -T\left(S^{o}_{f,B} - S^{o}_{f,A} + \int_{298K}^{T} \frac{\Delta C_{p,A\leftrightarrow B}}{T} dT\right)\end{aligned} \tag{S-1}$$

where $\Delta H^{o}_{f,A}, \Delta H^{o}_{f,B}$ and $S^{o}_{f,A}, S^{o}_{f,B}$ are the enthalpy and entropy of formation of components A and B at 298 K and 1 atm. $\Delta C_{p,A\leftrightarrow B}$ is the difference between the constant pressure heat capacities of component A and B at temperature T. The enthalpies and entropies of formation, and the constant pressure heat capacities of xylene isomers are obtained from Refs.[S7–S10] The Brick software[S11] uses the ideal gas partition function of each component as input. The reader is referred to the Supporting Information of Ref.[S11] for detailed steps for converting $\Delta G^{\text{ideal}}_{A\leftrightarrow B}$ to ideal gas partition functions. The values of $\Delta G^{\text{ideal}}_{A\leftrightarrow B}$ used in this work are listed in Table S4.

Table S4: Change of ideal gas free energy $\Delta G^{\text{ideal}}_{A\leftrightarrow B}$ of a reaction $A \leftrightarrow B$ at 523 K computed using tabulated data[S7–S10] for the reactions considered in this work.

Reaction A $\leftrightarrow$ B	$\Delta G^{\text{ideal}}_{A\leftrightarrow B}$ / [kJ/mol]
m-xylene $\leftrightarrow$ *o*-xylene	4.06
m-xylene $\leftrightarrow$ *p*-xylene	3.62

Multiple linear regression[S12,S13] is used to compute changes of enthalpy and entropy due to the transfer of one xylene molecule from the bulk phase (mixture of xylenes at chemical equilibrium) to the zeolite framework. The change of free energy $\Delta G_{\mathrm{tr},i}$ due to the transfer of one xylene molecule i from the bulk phase to the zeolite is related to the change of enthalpy $\Delta H_{\mathrm{tr},i}$ and entropy $\Delta S_{\mathrm{tr},i}$ by:

$$\Delta G_{\mathrm{tr},i} = \Delta H_{\mathrm{tr},i} - T\Delta S_{\mathrm{tr},i} \tag{S-2}$$

The change of free energy due to the transfer of one xylene molecule between the bulk phase and the zeolite is obtained using:[S14,S15]

$$\Delta G_{\mathrm{tr},i} = RT \ln \frac{\rho_{\mathrm{bulk},i}}{\rho_{\mathrm{ads},i}} \tag{S-3}$$

where $\rho_{\mathrm{bulk},i}$ and $\rho_{\mathrm{ads},i}$ are the number densities of molecule i in bulk phase and zeolite, respectively. The change of enthalpy $\Delta H_{\mathrm{tr},i}$ due to the transfer of one xylene molecule i from the bulk phase to the zeolite is obtained from:

$$\Delta H_{\mathrm{tr},i} = H_{\mathrm{ads},i} - H_{\mathrm{bulk},i} - RT \tag{S-4}$$

where $H_{\mathrm{ads},i}$ is the enthalpy of adsorption of component i from the mixture of xylenes at chemical equilibrium in the zeolite framework, and $H_{\mathrm{bulk},i}$ is the enthalpy of adsorption of component i in the bulk phase mixture of xylenes at chemical equilibrium. Both $H_{\mathrm{ads},i}$ and $H_{\mathrm{bulk},i}$ are computed by Monte Carlo simulations in the grand-canonical ensemble using multiple linear regression.[S12,S13]

The Brick-CFCMC software[S11] was used to compute fugacity coefficients ϕ_i for component i from the excess chemical potential $\mu_{\text{excess},i}$ obtained with the CFCMC method using:[S16]

$$\phi_i = \frac{N}{\beta V} \exp\left(\beta \mu_{\text{excess},i}\right) \tag{S-5}$$

where N is the total number of whole molecules, and V is the volume of the simulation box.

For the input for grand-canonical Monte Carlo simulations using the RASPA software,[S4,S17,S18] the fugacity coefficients are transformed to chemical potentials μ_i using:[S18]

$$\beta \mu_i = \beta \mu^0_{\text{IG},i} + \ln\left(\beta \phi_i P\right) \tag{S-6}$$

where P is the pressure, and $\mu^0_{\text{IG},i}$ is the the chemical potential of the reference state.

The selectivities $S_{\mathrm{A/B}}$ for the adsorption of component A over B from the bulk phase at chemical equilibrium in the zeolite types considered in this work are calculated using:[S19]

$$S_{\mathrm{A/B}} = \left(\frac{q_{\mathrm{A}}}{q_{\mathrm{B}}}\right)\left(\frac{x_{\mathrm{B}}}{x_{\mathrm{A}}}\right) \tag{S-7}$$

where q_i is the computed loading of component i in the zeolite framework; and x_i is the mole fraction of component i in the bulk phase mixture of xylenes at chemical equilibrium.

Table S5: Composition of the mixture of xylene isomers at chemical equilibrium, fugacity coefficients of xylenes, and density of the mixture as a function of pressure at 523 K as computed by Monte Carlo simulations in the *NPT*-ensemble, combined with the reaction ensemble. The numbers between round brackets denote the uncertainties in the last digit.

Pressure /	Mole fraction / [-]			Fugacity coefficient / [-]			Density /	State
[bar]	*m*-xylene	*o*-xylene	*p*-xylene	*m*-xylene	*o*-xylene	*p*-xylene	[kg/m^3]	of matter
0.03	0.547(2)	0.214(2)	0.239(2)	0.987(16)	0.994(24)	0.984(25)	0.073(1)	vapor
0.053	0.547(3)	0.215(2)	0.238(2)	0.986(18)	0.984(26)	0.992(10)	0.129(1)	vapor
0.094	0.547(2)	0.216(2)	0.237(3)	0.988(18)	0.985(15)	0.992(14)	0.230(1)	vapor
0.168	0.547(3)	0.215(2)	0.238(5)	0.979(28)	0.986(13)	0.972(17)	0.410(1)	vapor
0.3	0.547(2)	0.216(3)	0.237(2)	0.982(28)	0.989(13)	0.985(14)	0.730(1)	vapor
0.533	0.547(2)	0.216(3)	0.237(3)	0.981(29)	0.979(20)	0.978(20)	1.303(1)	vapor
0.94	0.546(1)	0.215(1)	0.239(2)	0.980(24)	0.976(14)	0.973(44)	2.333(1)	vapor
1.68	0.546(4)	0.215(2)	0.239(5)	0.971(27)	0.967(11)	0.961(18)	4.197(2)	vapor
3	0.547(3)	0.215(2)	0.238(3)	0.942(20)	0.946(18)	0.943(21)	7.625(4)	vapor
5.33	0.547(4)	0.214(4)	0.239(2)	0.913(18)	0.911(19)	0.903(11)	14.12(1)	vapor
16.87	0.536(10)	0.229(17)	0.235(11)	0.587(52)	0.544(33)	0.589(50)	623(2)	liquid
30	0.533(10)	0.225(10)	0.242(11)	0.348(18)	0.319(11)	0.338(16)	629(2)	liquid
53.3	0.539(9)	0.226(8)	0.235(11)	0.215(13)	0.203(12)	0.213(7)	640(3)	liquid
94.8	0.536(18)	0.231(14)	0.233(8)	0.140(12)	0.129(6)	0.139(8)	655(2)	liquid
168.7	0.530(19)	0.229(22)	0.241(16)	0.107(10)	0.098(7)	0.103(6)	677(2)	liquid
300	0.536(16)	0.229(22)	0.235(15)	0.090(6)	0.083(7)	0.090(3)	703(2)	liquid

Table S6: Heat of adsorption at infinite dilution of xylene isomers at 523 K in the zeolite framework types considered in this work as computed by Monte Carlo simulations via Widom's test-particle insertion method.[S20] The numbers between round brackets denote the uncertainties in the last digit.

Zeolite type	*m*-xylene / [kJ/mol]	*o*-xylene / [kJ/mol]	*p*-xylene / [kJ/mol]
FAU	40.865(3)	40.835(5)	40.540(6)
MWW	53.25(2)	60.4(3)	65.0(4)
AFI	56.236(9)	47.608(8)	57.205(5)
MEL	67.47(5)	62.99(6)	65.69(7)
MOR	62.285(1)	62.59(3)	62.951(9)
BEA	59.247(8)	58.63(1)	61.27(1)
MRE	50.0(8)	34.5(2)	71.97(4)
MFI	69.7(2)	56.5(5)	62.8(2)
MTW	65.82(4)	67.5(1)	68.43(4)

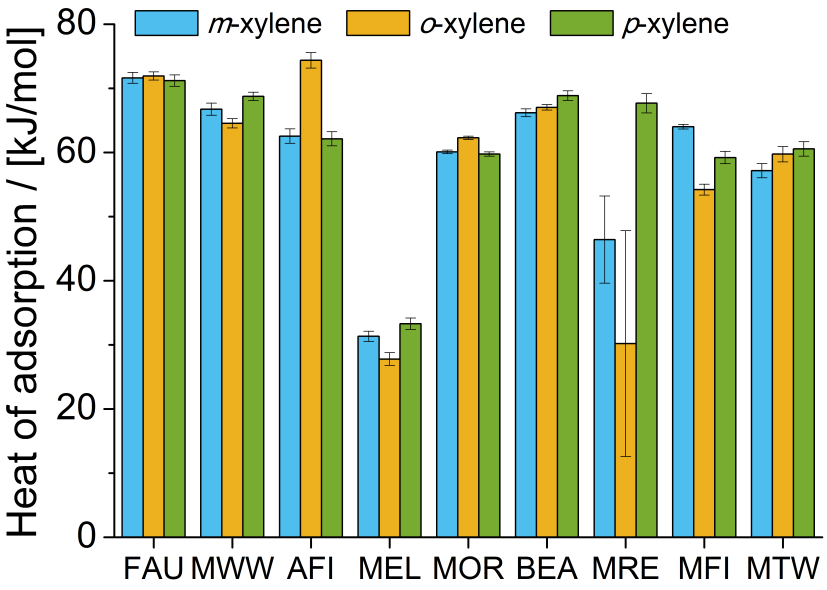

Figure S2: Heat of adsorption of xylene isomers at 523 K and 30 bar in the zeolite framework types considered in this work, adsorbed from the mixture at chemical equilibrium as computed by Monte Carlo simulations.

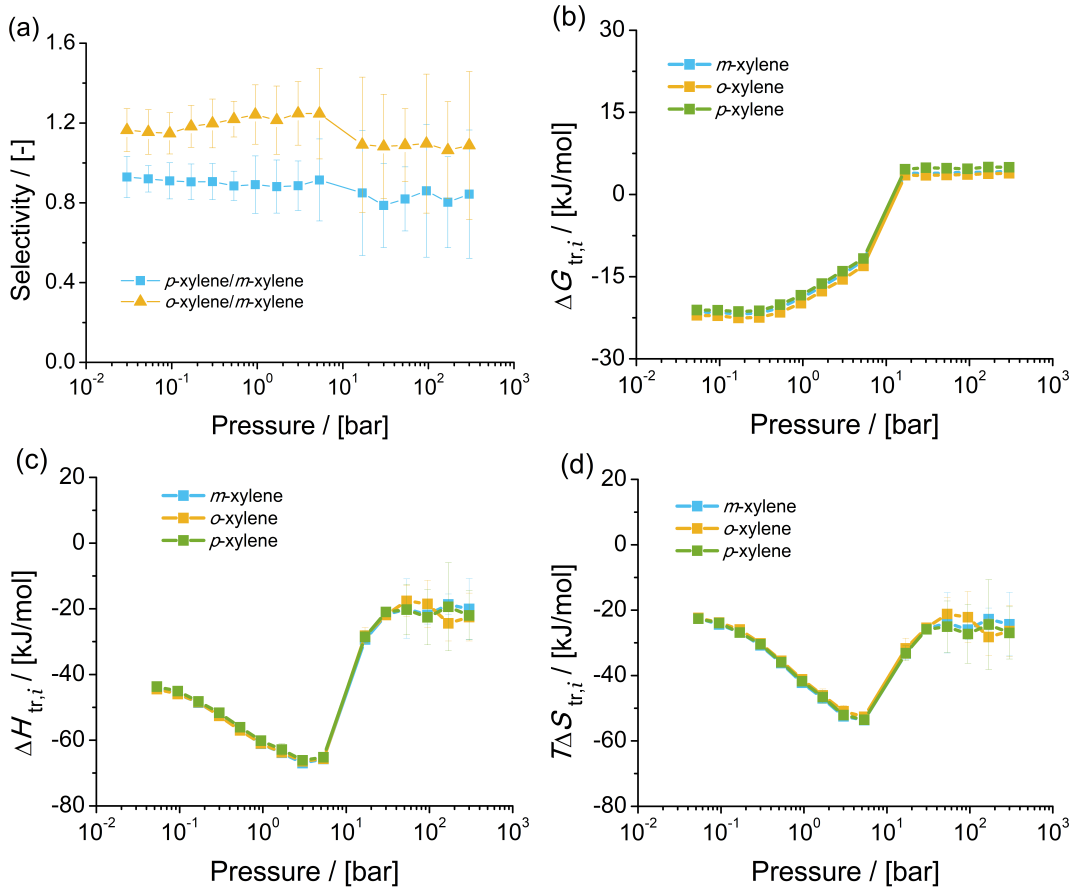

Figure S3: (a) Selectivities for the adsorption of xylenes from the bulk phase at chemical equilibrium at 523 K in FAU-type zeolite in the ternary mixture (computed using Eq. S-7); computed (b) changes in free energy $\Delta G_{\mathrm{tr},i}$, (c) changes in enthalpy $\Delta H_{\mathrm{tr},i}$, and (d) changes in entropy $T\Delta S_{\mathrm{tr},i}$, due to transferring one xylene molecule of type i from the bulk phase at chemical equilibrium to FAU-type zeolite at 523 K.

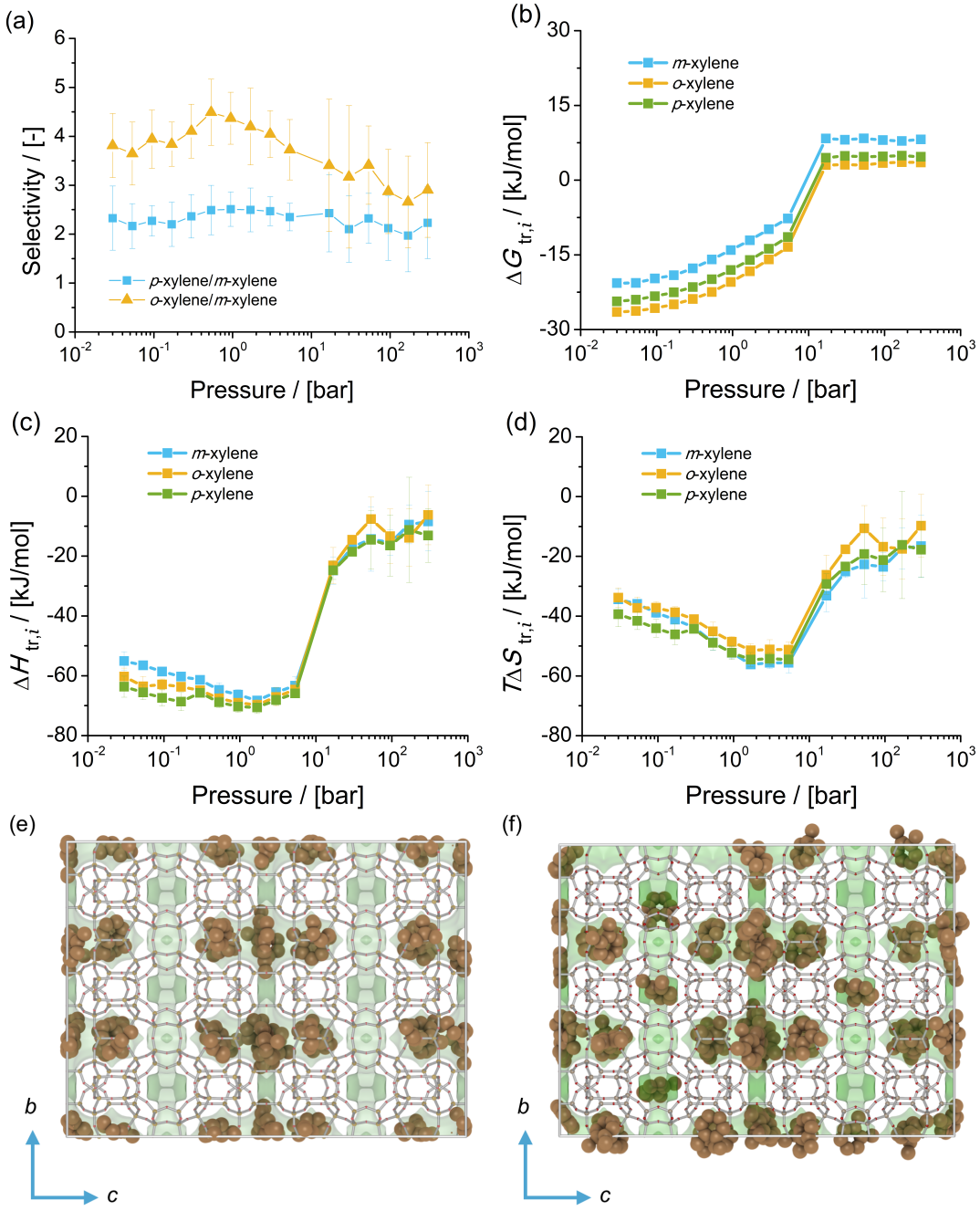

Figure S4: (a) Selectivities for the adsorption of xylenes from the bulk phase at chemical equilibrium at 523 K in MWW-type zeolite in the ternary mixture (computed using Eq. S-7); computed (b) changes in free energy $\Delta G_{\mathrm{tr},i}$, (c) changes in enthalpy $\Delta H_{\mathrm{tr},i}$, and (d) changes in entropy $T\Delta S_{\mathrm{tr},i}$, due to transferring one xylene molecule of type i from the bulk phase at chemical equilibrium to MWW-type zeolite at 523 K. Typical snapshots of the simulation of adsorption of pure *o*-xylene in MWW-type zeolite at 523 K and (e) 0.94 bar and (f) 300 bar. At 0.94 bar, *o*-xylene is only located in the 12-ring cages. At 300 bar, *o*-xylene is located both in the 12-ring cages and the 10-ring channels.

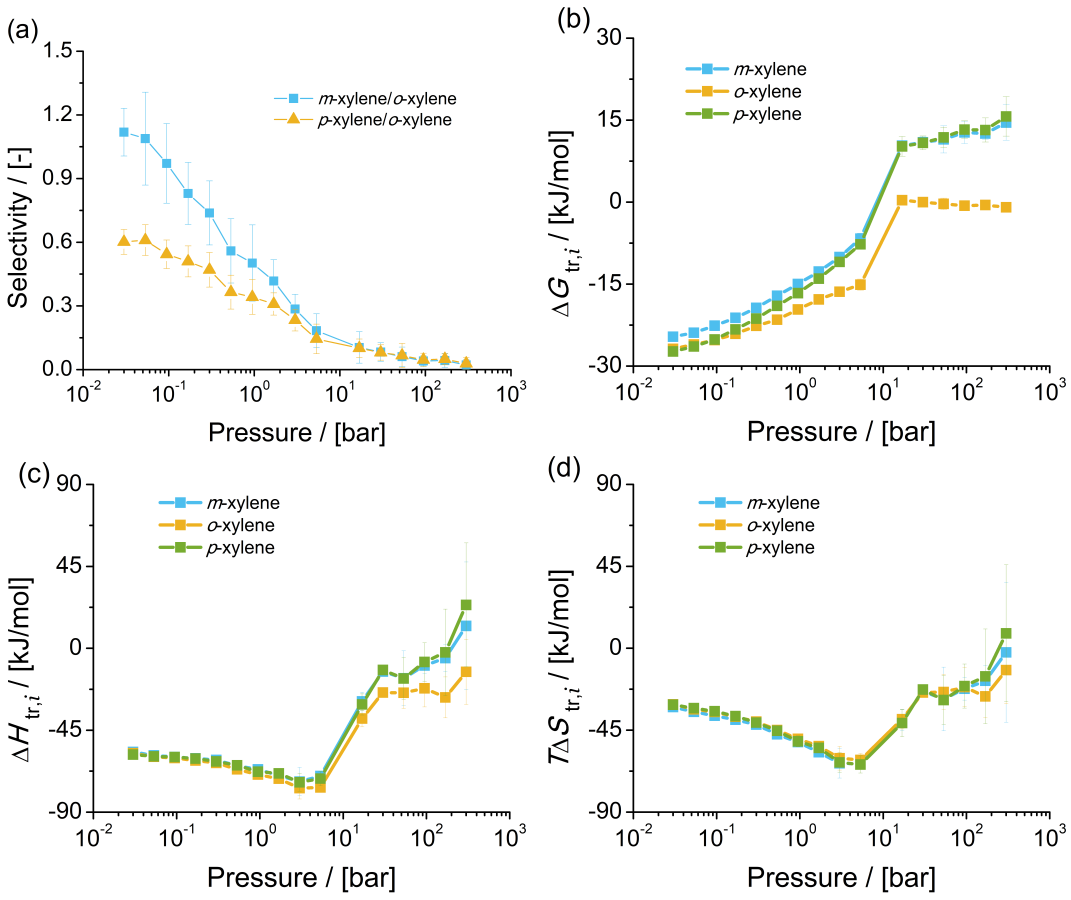

Figure S5: (a) Selectivities for the adsorption of xylenes from the bulk phase at chemical equilibrium at 523 K in AFI-type zeolite in the ternary mixture (computed using Eq. S-7); computed (b) changes in free energy $\Delta G_{\mathrm{tr},i}$, (c) changes in enthalpy $\Delta H_{\mathrm{tr},i}$, and (d) changes in entropy $T\Delta S_{\mathrm{tr},i}$, due to transferring one xylene molecule of type i from the bulk phase at chemical equilibrium to AFI-type zeolite at 523 K.

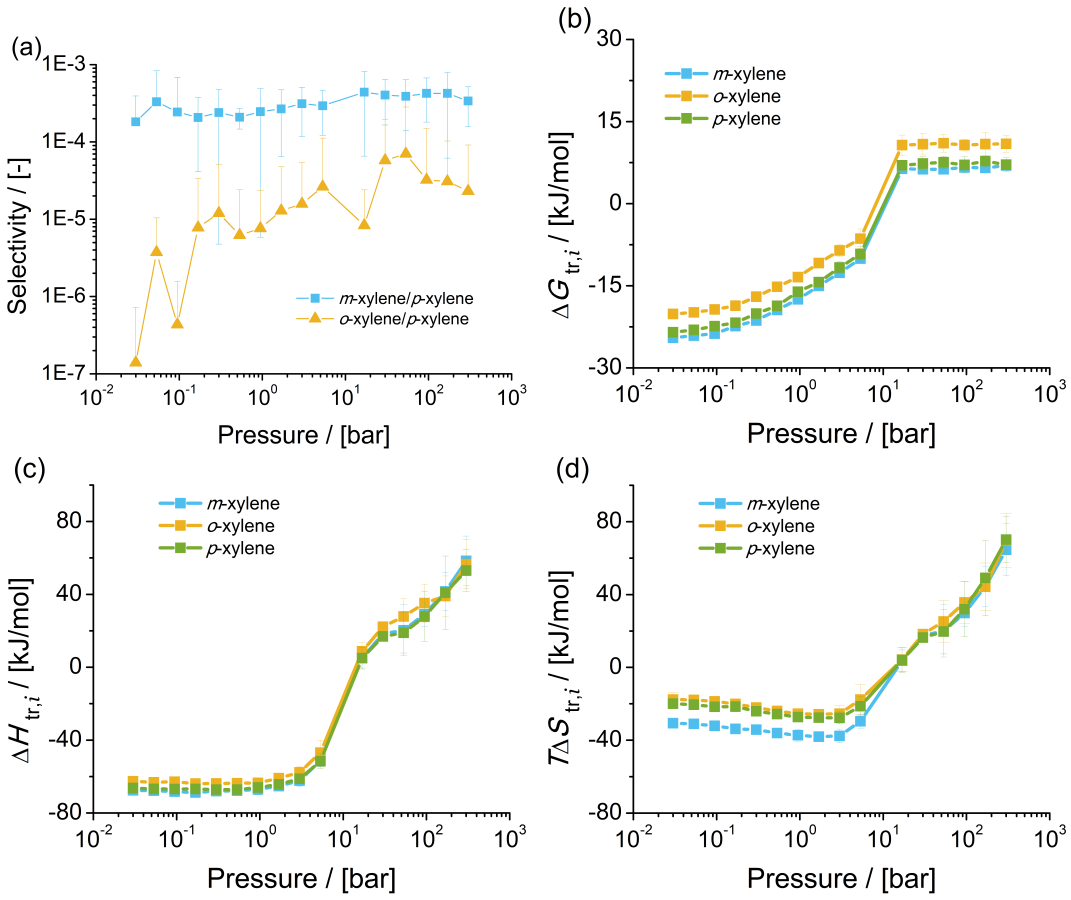

Figure S6: (a) Selectivities for the adsorption of xylenes from the bulk phase at chemical equilibrium at 523 K in MEL-type zeolite in the ternary mixture (computed using Eq. S-7); computed (b) changes in free energy $\Delta G_{\mathrm{tr},i}$, (c) changes in enthalpy $\Delta H_{\mathrm{tr},i}$, and (d) changes in entropy $T\Delta S_{\mathrm{tr},i}$, due to transferring one xylene molecule of type i from the bulk phase at chemical equilibrium to MEL-type zeolite at 523 K.

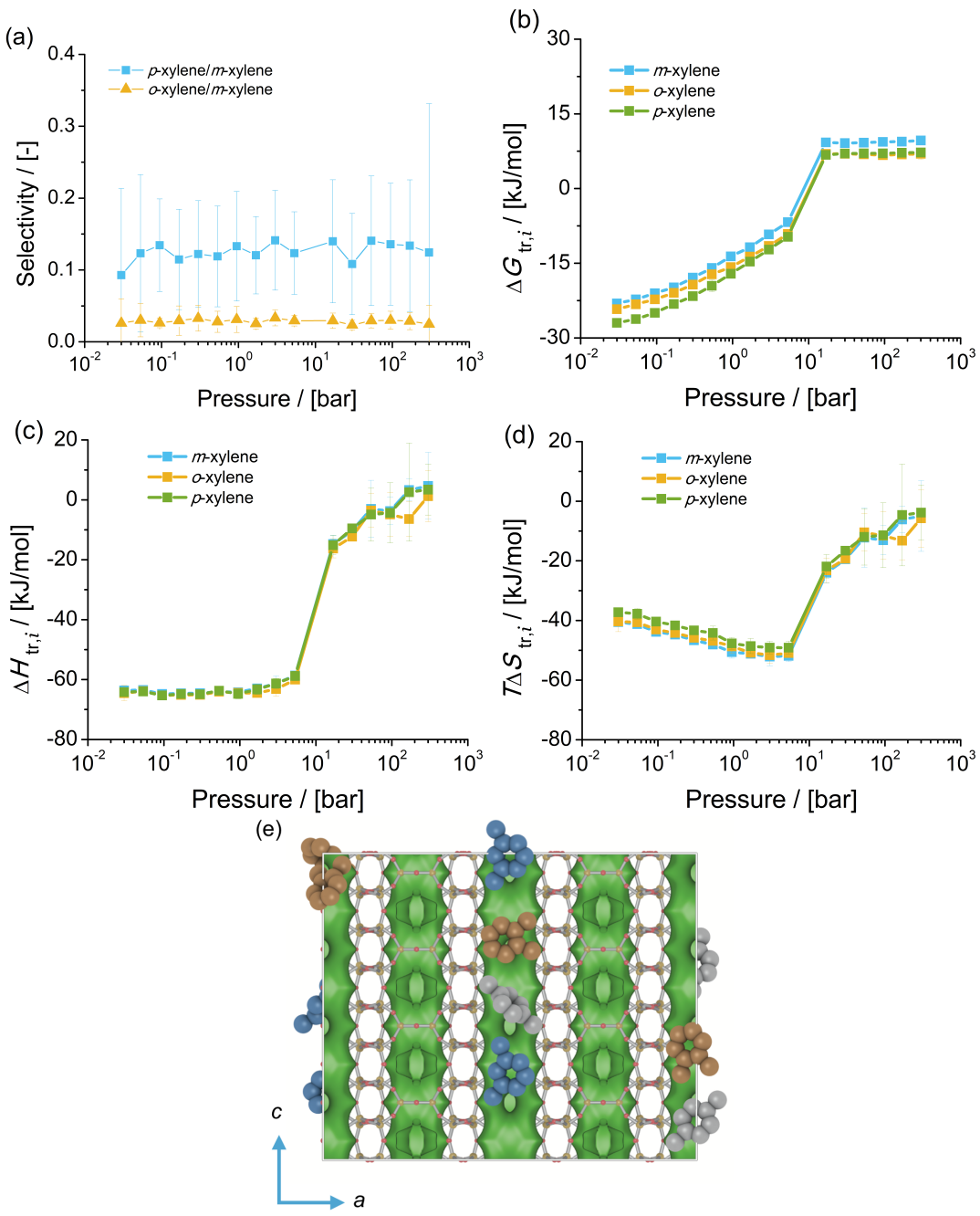

Figure S7: (a) Selectivities for the adsorption of xylenes from the bulk phase at chemical equilibrium at 523 K in MOR-type zeolite in the ternary mixture (computed using Eq. S-7); computed (b) changes in free energy $\Delta G_{\mathrm{tr},i}$, (c) changes in enthalpy $\Delta H_{\mathrm{tr},i}$, and (d) changes in entropy $T\Delta S_{\mathrm{tr},i}$, due to transferring one xylene molecule of type i from the bulk phase at chemical equilibrium to MOR-type zeolite at 523 K. (e) Typical snapshots of the simulation of adsorption of the mixture of xylene isomers in MOR-type zeolite at 300 bar and 523 K. *m*-Xylene is shown in blue, *p*-xylene in grey, and *o*-xylene in orange.

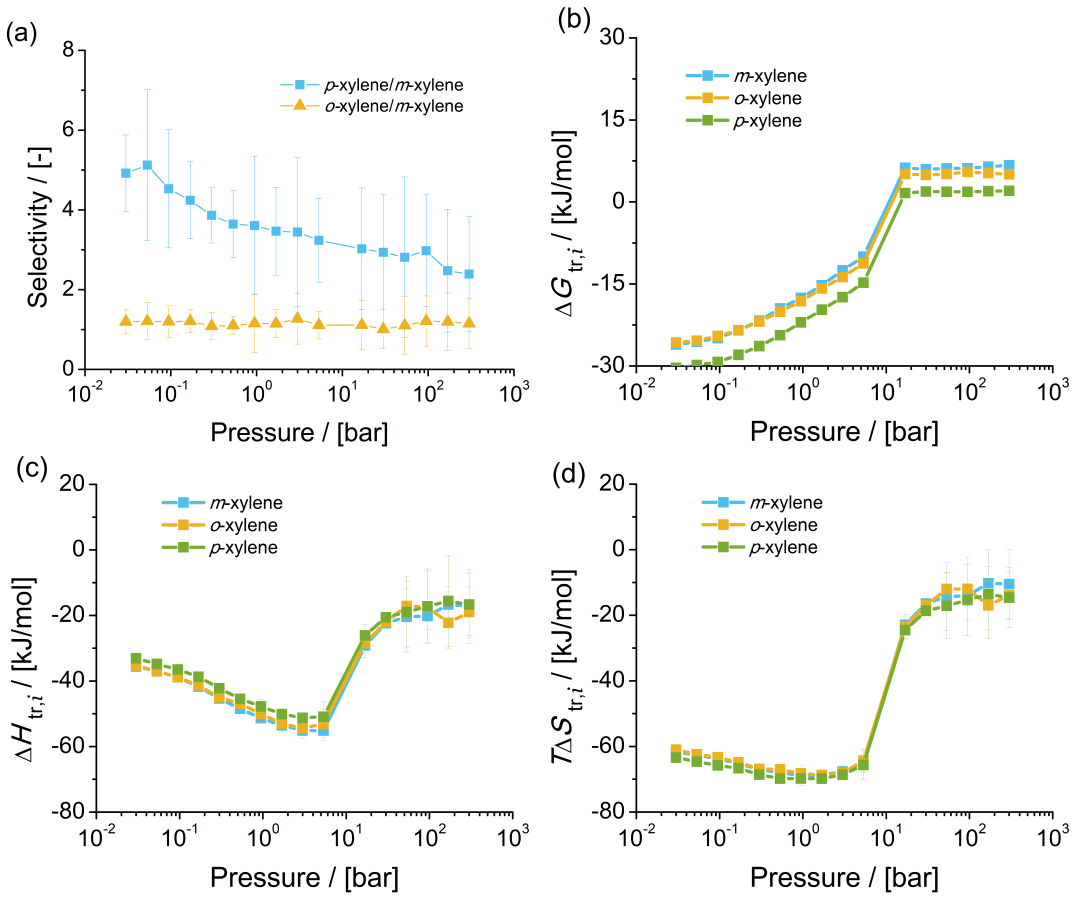

Figure S8: (a) Selectivities for the adsorption of xylenes from the bulk phase at chemical equilibrium at 523 K in BEA-type zeolite in the ternary mixture (computed using Eq. S-7); computed (b) changes in free energy $\Delta G_{\mathrm{tr},i}$, (c) changes in enthalpy $\Delta H_{\mathrm{tr},i}$, and (d) changes in entropy $T\Delta S_{\mathrm{tr},i}$, due to transferring one xylene molecule of type i from the bulk phase at chemical equilibrium to BEA-type zeolite at 523 K.

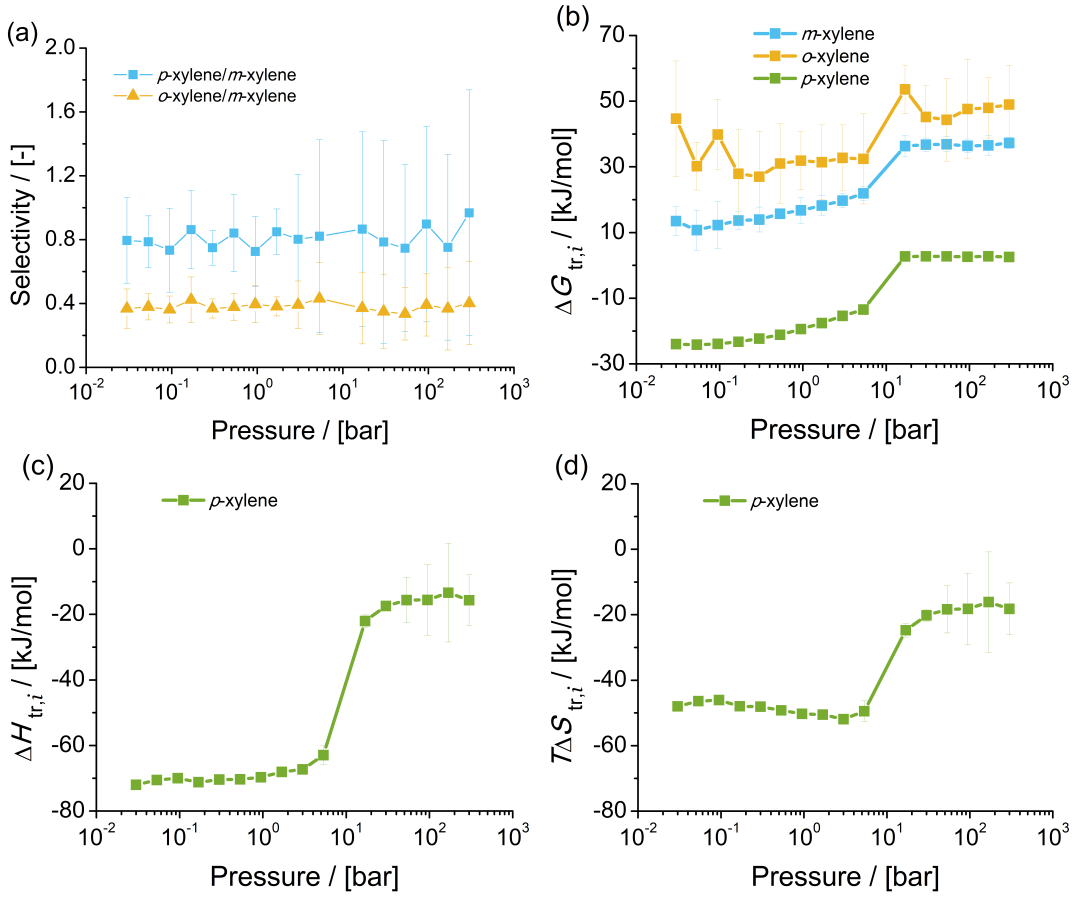

Figure S9: (a) Selectivities for the adsorption of xylenes from the bulk phase at chemical equilibrium at 523 K in MRE-type zeolite in the ternary mixture (computed using Eq. S-7); computed (b) changes in free energy $\Delta G_{\mathrm{tr},i}$, (c) changes in enthalpy $\Delta H_{\mathrm{tr},i}$, and (d) changes of entropy $T\Delta S_{\mathrm{tr},i}$, due to transferring one xylene molecule of type i from the bulk phase at chemical equilibrium to MRE-type zeolite at 523 K. Changes in enthalpy for m-xylene and o-xylene are not shown due to poor sampling of enthalpy of adsorption in the zeolite, as these molecules are not adsorbed by MRE-type zeolite.

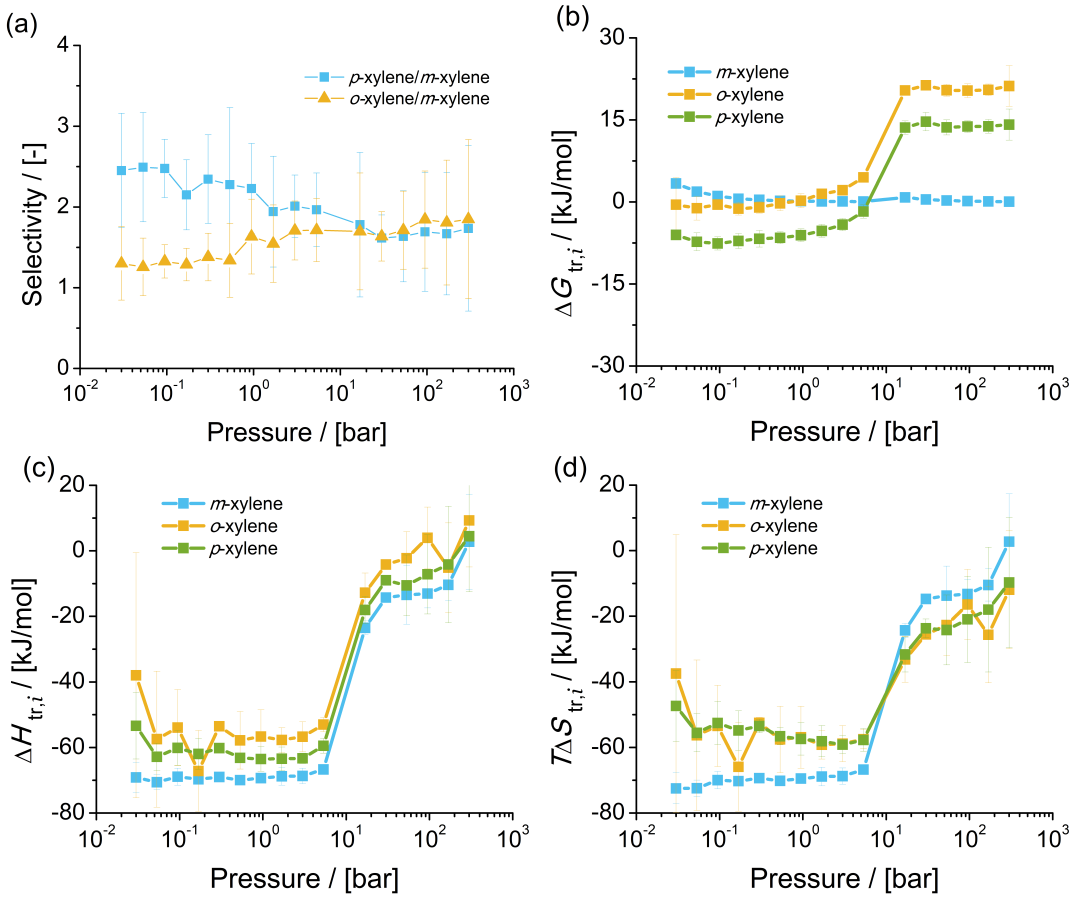

Figure S10: (a) Selectivities for the adsorption of xylenes from the bulk phase at chemical equilibrium at 523 K in MFI-type zeolite in the ternary mixture (computed using Eq. S-7); computed (b) changes in free energy $\Delta G_{\mathrm{tr},i}$, (c) changes in enthalpy $\Delta H_{\mathrm{tr},i}$, and (d) changes in entropy $T\Delta S_{\mathrm{tr},i}$, due to transferring one xylene molecule of type i from the bulk phase at chemical equilibrium to MFI-type zeolite at 523 K.

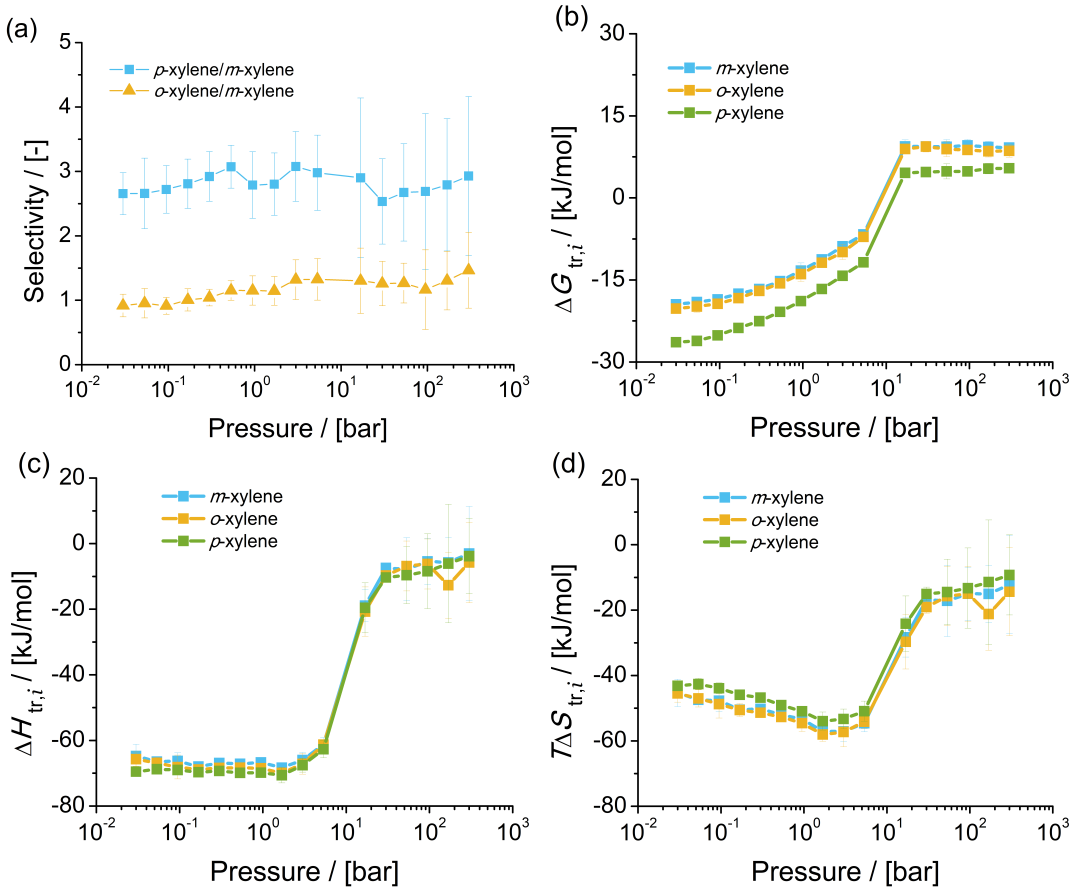

Figure S11: (a) Selectivities for the adsorption of xylenes from the mixture at chemical equilibrium at 523 K in MTW-type zeolite in the ternary mixture (computed using Eq. S-7); computed (b) changes in free energy $\Delta G_{\mathrm{tr},i}$, (c) changes in enthalpy $\Delta H_{\mathrm{tr},i}$, and (d) changes in entropy $T\Delta S_{\mathrm{tr},i}$, due to transferring one xylene molecule of type i from the bulk phase at chemical equilibrium to MTW-type zeolite at 523 K.

References

(S1) Wick, C. D.; Martin, M. G.; Siepmann, J. I. Transferable potentials for phase equilibria. 4. United-atom description of linear and branched alkenes and alkylbenzenes. *J. Phys. Chem. B* **2000**, *104*, 8008–8016.

(S2) Allen, M. P.; Tildesley, D. *Computer simulation of liquids*, 2nd ed.; Oxford University Press: Oxford, 2017.

(S3) Bai, P.; Tsapatsis, M.; Siepmann, J. I. TraPPE-zeo: Transferable potentials for phase equilibria force field for all-silica zeolites. *J. Phys. Chem. C* **2013**, *117*, 24375–24387.

(S4) Dubbeldam, D.; Calero, S.; Vlugt, T. J. H. iRASPA: GPU-accelerated visualization software for materials scientists. *Mol. Simulat.* **2018**, *44*, 653–676.

(S5) Baerlocher, C.; McCusker, L. B. Database of zeolite structures. `http://www.iza-structure.org/databases/`, Accessed: 04-05-2020.

(S6) Mullen, R. G.; Maginn, E. J. Reaction ensemble Monte Carlo simulation of xylene isomerization in bulk phases and under confinement. *J. Chem. Theory Comput.* **2017**, *13*, 4054–4062.

(S7) Prosen, E. J.; Johnson, W. H.; Rossini, F. D. Heats of combustion and formation at 25 degrees C of the alkylbenzenes through $C_{10}H_{14}$, and of the higher normal monoalkylbenzenes. *J. Res. Natl. Inst. Stan.* **1946**, *36*, 455–461.

(S8) Pitzer, K. S.; Scott, D. W. The thermodynamics and molecular structure of benzene and its methyl derivatives. *J. Am. Chem. Soc.* **1943**, *65*, 803–829.

(S9) Draeger, J. A. The methylbenzenes II. Fundamental vibrational shifts, statistical thermodynamic functions, and properties of formation. *J. Chem. Thermodyn.* **1985**, *17*, 263 – 275.

(S10) Chao, J.; Hall, K. R.; Marsh, K. N.; Wilhoit, R. C. Thermodynamic properties of key organic oxygen compounds in the carbon range C_1 to C_4. Part 2. Ideal gas properties. *J. Phys. Chem. Ref. Data* **1986**, *15*, 1369–1436.

(S11) Hens, R.; Rahbari, A.; Caro-Ortiz, S.; Dawass, N.; Erdős, M.; Poursaeidesfahani, A.; Salehi, H. S.; Celebi, A. T.; Ramdin, M.; Moultos, O. A.; Dubbeldam, D.; Vlugt, T. J. H. Brick-CFCMC: Open source software for Monte Carlo simulations of phase and reaction equilibria using the Continuous Fractional Component Method. *J. Chem. Inf. Model.* **2020**, *60*, 2678–2682.

(S12) Josephson, T. R.; Singh, R.; Minkara, M. S.; Fetisov, E. O.; Siepmann, J. I. Partial molar properties from molecular simulation using multiple linear regression. *Mol. Phys.* **2019**, *117*, 3589–3602.

(S13) Rahbari, A.; Josephson, T. R.; Sun, Y.; Moultos, O. A.; Dubbeldam, D.; Siepmann, J. I.; Vlugt, T. J. Multiple linear regression and thermodynamic fluctuations are equivalent for computing thermodynamic derivatives from molecular simulation. *Fluid Phase Equilibr.* **2020**, *523*, 112785.

(S14) Martin, M. G.; Siepmann, J. I. Calculating Gibbs free energies of transfer from Gibbs ensemble Monte Carlo simulations. *Theor. Chem. Acc.* **1998**, *99*, 347–350.

(S15) Ben-Naim, A. *Statistical thermodynamics for chemists and biochemists*, 1st ed.; Plenum Press: New York, 1992.

(S16) Rahbari, A. Thermodynamics of Industrially Relevant Systems. Ph.D. thesis, Delft University of Technology, 2020.

(S17) Dubbeldam, D.; Calero, S.; Ellis, D. E.; Snurr, R. Q. RASPA: molecular simulation software for adsorption and diffusion in flexible nanoporous materials. *Mol. Simulat.* **2016**, *42*, 81–101.

(S18) Dubbeldam, D.; Torres-Knoop, A.; Walton, K. S. On the inner workings of Monte Carlo codes. *Mol. Simulat.* **2013**, *39*, 1253–1292.

(S19) Krishna, R. Screening metal–organic frameworks for mixture separations in fixed-bed adsorbers using a combined selectivity/capacity metric. *RSC Adv.* **2017**, *7*, 35724–35737.

(S20) Widom, B. Some topics in the theory of fluids. *J. Chem. Phys.* **1963**, *39*, 2808–2812.